

# Developments in g-C<sub>3</sub>N<sub>4</sub>-based nanomaterial-based photocatalytic hydrogen generation and photocatalytic ion doping

Shengwei Guo<sup>a</sup>, Yifeng Chai<sup>b,\*</sup>

School of Physics and Electronic Science, Hunan University of Science and Technology, Xiangtan, China  
<sup>a</sup>18803409478@163.com, <sup>b</sup>yfc@hnust.edu.cn

\*Corresponding author

**Abstract:** The scientific advancement on g-C<sub>3</sub>N<sub>4</sub> in the areas of hydrogen generation and ion doping is the main topic of this study. The modification techniques of graphitic phase carbon nitride are elaborated to improve the photocatalytic hydrogen precipitation efficiency of g-C<sub>3</sub>N<sub>4</sub> through elemental doping, structural modulation, and heterojunction construction. These techniques aim to address the drawbacks of graphitic phase carbon nitride, including small specific surface area, fast photogenerated carrier complexation, and low visible light utilization efficiency. The effects of ion doping on g-C<sub>3</sub>N<sub>4</sub>'s photocatalytic performance are also thoroughly examined in this paper, along with the correlation between doping type, concentration, and photocatalytic activity. The thorough analysis demonstrates that ion doping is a useful strategy for maximizing g-C<sub>3</sub>N<sub>4</sub>'s photocatalytic performance, and although g-C<sub>3</sub>N<sub>4</sub>'s potential for hydrogen generation is evident, more investigation and development are still required. The purpose of this review is to offer scholars working in related subjects useful references and advice.

**Keywords:** Ion doping; G-C<sub>3</sub>N<sub>4</sub> photocatalytic generation of Hydrogen; Degradation of pollutants

## 1. Introduction

g-C<sub>3</sub>N<sub>4</sub> shows a special photocatalytic hydrolysis for hydrogen generation when exposed to visible light. In particular, electrons in the catalyst's valence band (VB) migrate to the conduction band (CB) upon absorbing sufficient energy, whereupon they get excited and move towards the catalyst surface. Here, they combine with the water molecules in a reduction process to create hydrogen. Recombination of electrons and holes, however, is a crucial component of the photocatalytic process<sup>[1]</sup>(shown in Fig 1). The excited electrons and holes are consumed by this recombination process, which lowers the photocatalytic efficiency. Furthermore, g-C<sub>3</sub>N<sub>4</sub>'s shape and prohibited band width both significantly impact the catalytic action. Researchers often use changes, such as doping of metallic or nonmetallic elements and morphological modulation, to enhance the electrical structure and optical characteristics of g-C<sub>3</sub>N<sub>4</sub> in order to increase its hydrogen precipitation efficiency. The objective of these modification efforts is to raise the photocatalytic activity of g-C<sub>3</sub>N<sub>4</sub> by decreasing the rate at which electron-hole pairs recombine and increasing the separation efficiency of photogenerated carriers. We hope that these initiatives will advance the area of solar hydrogen production.

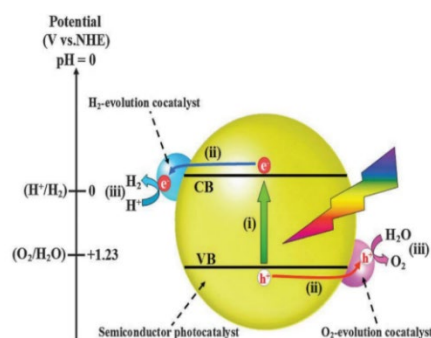


Figure 1: Schematic illustration of photocatalytic water splitting over a photocatalyst loaded with H<sub>2</sub> and O<sub>2</sub> evolution co-catalysts valence band of various semiconductor.<sup>[1]</sup>

## 2. Optimization of performance of g-C<sub>3</sub>N<sub>4</sub>

Finding novel and effective photocatalysts is essential to using solar energy to address energy and environmental issues. A well-liked catalyst for photocatalytic hydrogen precipitation, g-C<sub>3</sub>N<sub>4</sub>, exhibits considerable application potential. However, its rate of hydrogen creation is very low, nearly insignificant, because to the fast complexation of photogenerated electrons and holes. We used a co-catalyst for g-C<sub>3</sub>N<sub>4</sub> modification in order to improve it. Bi Ling et al<sup>[2]</sup>, used PtCo<sub>x</sub> co-catalyst. According to the experimental findings, PtCo<sub>x</sub>'s higher electrical conductivity aided in the PtCo<sub>x</sub>/g-C<sub>3</sub>N<sub>4</sub> photocatalysts' enhanced photogenerated charge migration and separation efficiency, while PtCo<sub>x</sub>'s overpotential quickened the reaction kinetics (Fig. 2). Using a straightforward solvothermal technique, the PtCo<sub>x</sub> bimetallic co-catalyst was effectively loaded onto the g-C<sub>3</sub>N<sub>4</sub> surface. 2.5 PtCo<sub>x</sub> shown enhanced photocatalytic activity, releasing hydrogen at a rate of 11.9 μmol/h/g. PtCo<sub>x</sub>/g-C<sub>3</sub>N<sub>4</sub> photocatalysts' photogenerated charge behavior was methodically examined and described using surface photovoltage, transient surface photovoltage, surface photocurrent, and photoacoustic methods. This work advances the theoretical understanding necessary to fabricate co-catalyst/photocatalyst systems in the future and enhances the photocatalytic performance of g-C<sub>3</sub>N<sub>4</sub>.

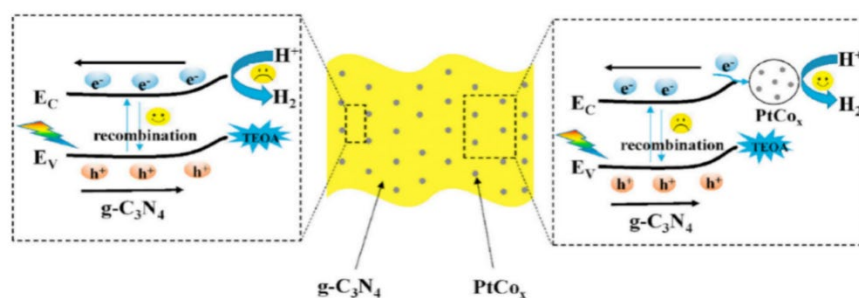


Figure 2: Proposed mechanism of separation and transfer of photogenerated charge carriers at the interface between g-C<sub>3</sub>N<sub>4</sub> and PtCo<sub>x</sub><sup>[2]</sup>.

High atom utilization and a well-defined coordination structure in single-atom catalyst technology offer a fresh approach to high-performance photocatalyst design, which also helps to minimize the need for precious metal co-catalysts. A range of single-atom Ru, Co, or Ni-modified MoS<sub>2</sub> (SA-MoS<sub>2</sub>)-based co-catalysts were developed and synthesized by Han Xin et al<sup>[3]</sup>. to enhance the efficacy of g-C<sub>3</sub>N<sub>4</sub> nanosheets (NS) photocatalytic hydrogen generation. The optimized Ru1-MoS<sub>2</sub>/g-C<sub>3</sub>N<sub>4</sub> photocatalysts had the highest hydrogen production rate of 1115 μmol/h/g, which is approximately 37 and 5 times higher than that of pure g-C<sub>3</sub>N<sub>4</sub> and MoS<sub>2</sub>/g-C<sub>3</sub>N<sub>4</sub> photocatalysts, respectively (Fig.3). The 2D SA-MoS<sub>2</sub>/g-C<sub>3</sub>N<sub>4</sub> photocatalysts containing single atoms of Ru, Co, or Ni showed similarly enhanced photocatalytic activity. The enhanced photocatalytic performance is primarily ascribed to the tight interface and synergistic effect between SA-MoS<sub>2</sub> and g-C<sub>3</sub>N<sub>4</sub> NSS with well-defined ligand monoatomic structures, which facilitates the fast interfacial charge transfer. Additionally, the altered electronic structure of the unique monoatomic structure of SA, MoS<sub>2</sub>, and suitable hydrogen adsorption properties that provide improved photocatalytic hydrogen production performance with abundant active sites are also noteworthy. These findings are supported by both experimental and density-functional theory calculations. A novel approach to enhance single-atom MoS<sub>2</sub>'s co-catalytic hydrogen generation efficiency is presented.

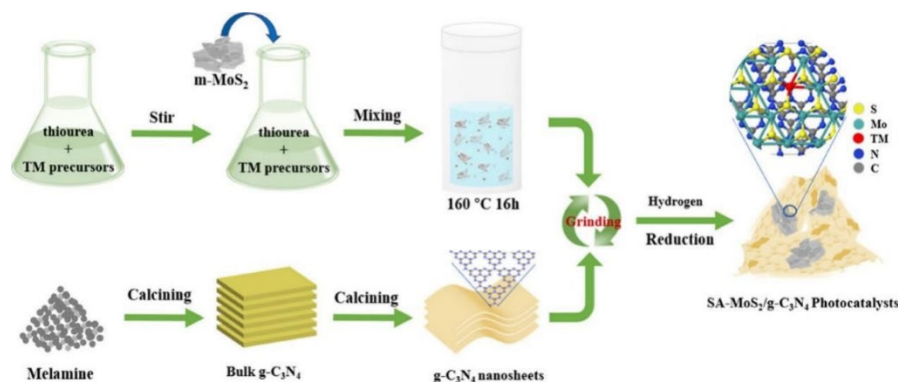


Figure 3: Schematic Diagram of the Synthetic Process of SA-MoS<sub>2</sub>/g-C<sub>3</sub>N<sub>4</sub> Photocatalysts with the Single-Atomic Structure<sup>[3]</sup>

The efficient conversion of solar energy into hydrogen ( $H_2$ ) energy has faced certain challenges since there are occasionally insufficiently good catalysts and efficient catalytic processes. Using a one-step hot water technique, Pan <sup>J</sup>[4] et al (Fig.4). synthesized three-dimensional/two-dimensional (3D/2D) CuS/g- $C_3N_4$  photocatalysts. In order to realize the near-infrared (NIR) light-induced photothermal effect, snowflake-like CuS embedded in graphitic carbon nitride (g- $C_3N_4$ ) nanosheets generated a heterojunction interface favorable to hydrogen production, accelerated charge transfer and segregation, and decreased the charge transfer distance. Because of the powerful influence of NIR-induced PTE, the (3D/2D) CuS/g- $C_3N_4$  catalyst demonstrated the highest hydrogen precipitation rate of 1422  $\mu\text{mol/h/g}$  at dual wavelengths of 420+850 nm and moderate hydrogen precipitation rate at 420 nm, respectively, which were 12 and 9 times higher than that of pure g- $C_3N_4$ . It is anticipated that near-infrared enhanced photocatalysis may be employed in a variety of thermally aided degradation processes by creating multifunctional composites with exceptional PTE and photocatalytic properties.

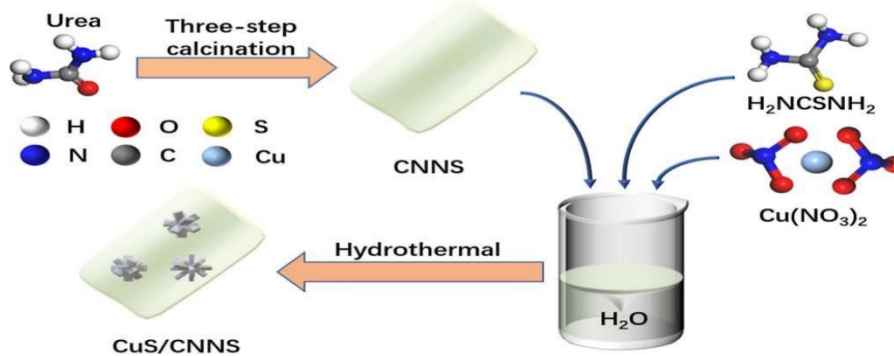


Figure 4: Schematic diagram of the preparation process for CuS/CNNS composites<sup>[4]</sup>.

Yan P. et al<sup>[5]</sup>. created a composite material made of graphitic phase carbon nitride (g- $C_3N_4$ ) and  $NaLiTi_3O_7$  in order to maximize the use of UV and visible light and to increase the separation efficiency of photogenerated carriers. XRD, SEM, TEM, XPS, FT-IR, UV-DRS, and TGA were used to describe the morphology and microstructure of the  $NaLiTi_3O_7$ /g- $C_3N_4$  photocatalyst. As seen in Fig. 5, the XRD and SEM data demonstrated that the well-crystallized  $NaLiTi_3O_7$  nanoparticles were evenly distributed over the surface of the g- $C_3N_4$  lamella and that the addition of g- $C_3N_4$  successfully reduced the agglomeration of  $NaLiTi_3O_7$  nanoparticles. Results from uV-DRS further demonstrated a significant redshift of the light absorption edge of the  $NaLiTi_3O_7$ /g- $C_3N_4$  composites. These benefits contribute to the good photocatalytic activity of the  $NaLiTi_3O_7$ /g- $C_3N_4$  composites. Under solar radiation, all  $NaLiTi_3O_7$ /g- $C_3N_4$  samples shown significantly superior hydrogen precipitation capabilities compared to pure g- $C_3N_4$  and  $NaLiTi_3O_7$ . The best  $NaLiTi_3O_7$ /g- $C_3N_4$  composite had 18 times more hydrogen precipitation than pure  $NaLiTi_3O_7$  and 4 times more than pure g- $C_3N_4$ . Because a heterojunction interface forms between them, allowing for the efficient separation of photogenerated electrons and holes over a larger light absorption range, coupling  $NaLiTi_3O_7$  with g- $C_3N_4$  greatly enhances photocatalytic performance when compared with pure  $NaLiTi_3O_7$  or g- $C_3N_4$ .

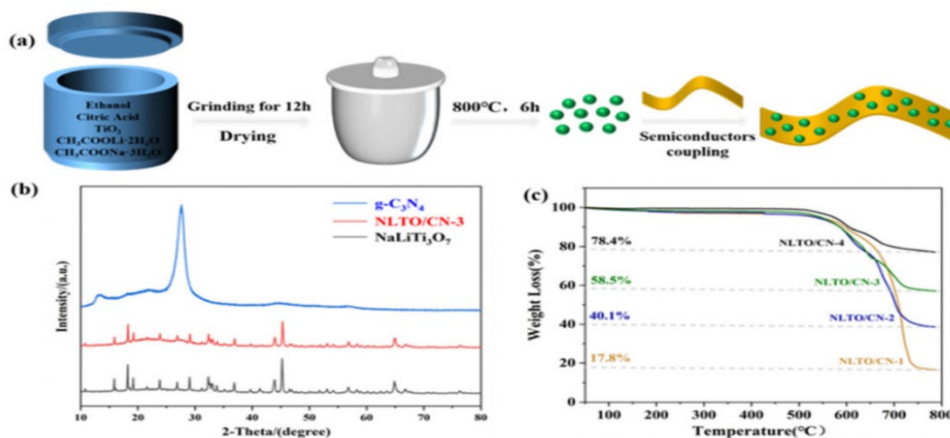


Figure 5: (a) Schematic diagram of the preparation of the photocatalysts<sup>[5]</sup>, (b) XRD patterns of pure  $NaLiTi_3O_7$  and pure g- $C_3N_4$ , and NLTO/CN-3<sup>[5]</sup>, (c) TG of  $NaLiTi_3O_7$ /g- $C_3N_4$  samples<sup>[5]</sup>.

### 3. Modification of g-C<sub>3</sub>N<sub>4</sub> by ionic doping

Semiconductors' electron configuration and band-edge potentials, which control the photocatalytic redox process, are the fundamental components of their photocatalytic activity. The range of light absorption and the possibility for redox reactions in a material are determined by the Fermi energy levels, which are directly correlated with the potentials of a semiconductor's valence band (VB) and conduction band (CB) as well as the bandgap energy between. One useful modification technique to greatly improve the performance of g-C<sub>3</sub>N<sub>4</sub> photocatalysts is ion doping. It is possible to modify the electronic structure, energy band structure, and light absorption characteristics of g-C<sub>3</sub>N<sub>4</sub> and hence increase its photocatalytic activity by adding metal and non-metal ions to the lattice. Ion doping, on the other hand, considerably increases the photocatalytic effectiveness by introducing additional active sites and encouraging the migration and separation of photogenerated electron-hole pairs.

#### 3.1. Metal ions doping

One major way to improve g-C<sub>3</sub>N<sub>4</sub>'s photocatalytic activity is by metal ion doping. Between g-C<sub>3</sub>N<sub>4</sub> and metal ions, heterojunctions can develop. Heterojunction can encourage photogenerated electron and hole separation and lessen the likelihood of their recombination. Furthermore, metal ions are added to the g-C<sub>3</sub>N<sub>4</sub> lattice to create defect states. These unique electronic states have the ability to capture and immobilize photogenerated electrons and holes, therefore delaying their premature recombination. Because of their distinct electrical structures, transition metal elements including cobalt, manganese, iron, and zinc are frequently employed as dopants. As they integrate into the g-C<sub>3</sub>N<sub>4</sub> structure, their d-orbital electrons can interact with the host material's to modify its energy band structure, enabling an increase in the range of light absorption and encouraging the migration and separation of photogenerated carriers. When combined, these factors greatly increase g-C<sub>3</sub>N<sub>4</sub>'s photocatalytic activity, offering compelling evidence for its use in environmental remediation and energy conversion applications.

Scheme heterojunction systems can be developed to increase the effectiveness of segregating and conveying charge carriers that are in charge of degrading contaminants. Thus, Hai T<sup>[6]</sup> used a straightforward technique to mix ZnCo<sub>2</sub>O<sub>4</sub> with g-C<sub>3</sub>N<sub>4</sub> to produce a novel Z-scheme heterogeneous nanocomposite. Using a variety of methods, the photocatalysts' nodularity, morphology, chemical composition, functional groups, energy band structure, and electrochemical characteristics were investigated. The catalytic activity of the g-C<sub>3</sub>N<sub>4</sub>/ZnCo<sub>2</sub>O<sub>4</sub> nanocomposites was much higher than that of the separate structural units (g-C<sub>3</sub>N<sub>4</sub>: $(45.7 \times 10^{-4} \text{ min}^{-1})$  and ZnCo<sub>2</sub>O<sub>4</sub>: $(79.5 \times 10^{-4} \text{ min}^{-1})$ ), as demonstrated by the photocatalytic degradation of methylene blue. When the pH was set to 7, the dosage of MB was 5 ppm, the photocatalyst was 90 mg of g-C<sub>3</sub>N<sub>4</sub>/ZnCo<sub>2</sub>O<sub>4</sub>, and the degradation rate of MB was up to 99% (Fig. 6). The photoluminescence and electrochemical impedance spectroscopy findings demonstrated that the photocatalytic efficacy of the nanocomposites was enhanced by the notable attenuation of the resultant electron-hole pair composite. Moreover, the two semiconductors' modified energy band structures and broad absorption of solar light led to a rise in photocatalytic activity.

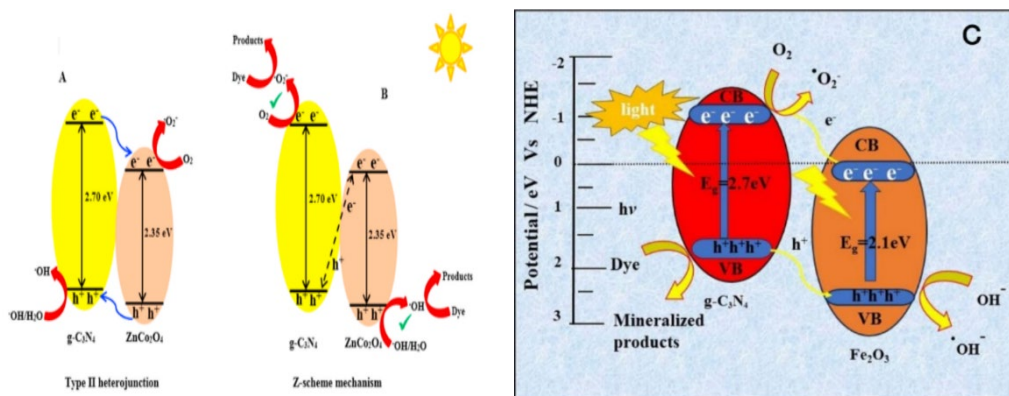


Figure 6: (A)(B)The MB degradation mechanism over g-CN/ZCO system<sup>[6]</sup>. (C)Possible photocatalytic degradation mechanism for the  $\alpha$ -Fe<sub>2</sub>O<sub>3</sub>/g-C<sub>3</sub>N<sub>4</sub> nanocomposite under visible light irradiation<sup>[7]</sup>.

Bharathi et al<sup>[7]</sup>, prepared Fe<sub>2</sub>O<sub>3</sub>/g-C<sub>3</sub>N<sub>4</sub> nanocomposites by in-situ pyrolysis (shown in Fig. 6). The structural, optical and morphological characteristics of the samples were investigated. FTIR studies confirmed the hybridization of C and N bonds in g-C<sub>3</sub>N<sub>4</sub> and Fe-O stretching vibrations in the Fe<sub>2</sub>O<sub>3</sub>/g-C<sub>3</sub>N<sub>4</sub> nanocomposites. seM studies showed that the g-C<sub>3</sub>N<sub>4</sub> nanosheets were combined with Fe<sub>2</sub>O<sub>3</sub>



crystals to form a distinct interface. XPS analysis of the 0.5-Fe<sub>2</sub>O<sub>3</sub>/g-C<sub>3</sub>N<sub>4</sub> nanocomposites reveals the chemical bonding states of the constituent elements. It was shown that the hybridization of Fe<sub>2</sub>O<sub>3</sub> and g-C<sub>3</sub>N<sub>4</sub> successfully separated the photogenerated carriers. The photocatalytic properties of the nanocomposites were investigated under visible light irradiation with methylene blue as the degradation object. The photocatalytic degradation efficiency of the nano 0.5-Fe<sub>2</sub>O<sub>3</sub>/g-C<sub>3</sub>N<sub>4</sub> composites reached 89% under 75 min of light irradiation.

### 3.2. Non-metal ion doping

By altering the locations of the conduction and valence bands, non-metallic ion doping mostly modifies the energy band structure of g-C<sub>3</sub>N<sub>4</sub>. Doped nonmetallic materials have the ability to decrease the band gap and introduce new energy levels in g-C<sub>3</sub>N<sub>4</sub>, increasing its light absorption range and improving its responsiveness to visible light. A desirable outcome has been the formation of highly active heterojunction photocatalysts with g-C<sub>3</sub>N<sub>4</sub> by nonmetallic doping. Photogenerated carriers are more mobile and easier to separate when doped with nonmetal ions like B, C, N, S, P, and O. under order to sustain g-C<sub>3</sub>N<sub>4</sub>'s strong photocatalytic activity under challenging conditions, non-metal doping also increases the stability of the compound.

Since almost half of sunlight is infrared (IR), it is important to investigate IR-responsive materials for photoelectrochemical water breakdown processes. Using a straightforward sintering technique, Fang Wu<sup>[8]</sup> et al (Fig.7). successfully synthesized phosphorus-doped g-C<sub>3</sub>N<sub>4</sub>, which demonstrated a 1.4 μA/cm<sup>2</sup> IR photoresponse when exposed to near-infrared (>800nm) light at 1.2V. At 0.6V, P/g-C<sub>3</sub>N<sub>4</sub> as a photoanode generated 1.27 μmol/h/g hydrogen, but the g-C<sub>3</sub>N<sub>4</sub> photocathode detected very little H<sub>2</sub>. This is explained by the introduction of P into g-C<sub>3</sub>N<sub>4</sub>, which causes the band gap to narrow from 2.75 eV to 1.37 eV and produces the superior IR photoresponse. Furthermore, P doping greatly enhanced the charge transfer and separation in g-C<sub>3</sub>N<sub>4</sub>.

N-doped TiO<sub>2</sub>/g-C<sub>3</sub>N<sub>4</sub> composites (also known as N-TiO<sub>2</sub>/g-C<sub>3</sub>N<sub>4</sub>) were created by Jiang G et al<sup>[9]</sup>(Fig.7). using a straightforward three-step procedure that maximized the heterojunction effect by evenly dispersing N-TiO<sub>2</sub> nanosheets across the g-C<sub>3</sub>N<sub>4</sub> layer. The photocatalytic elimination of ppb-level NO from continuous gas streams under visible light irradiation of this resultant composite was effective and long-lasting. g-C<sub>3</sub>N<sub>4</sub> could remove up to 46.1% of NO at this period. The photocatalytic removal of NO from N-TiO<sub>2</sub> was correlated with its content, with an ideal value of 25 mg/0.25 g. Through photocatalytic oxidation of NO by N-TiO<sub>2</sub>/g-C<sub>3</sub>N<sub>4</sub>, mechanistic studies demonstrated that N doping and the heterojunction structure of N-TiO<sub>2</sub>/g-C<sub>3</sub>N<sub>4</sub> enhanced the utilization of visible light and the reaction pathway of photoexcited electrons. The findings suggested that NO could be fully mineralized to nitrate.

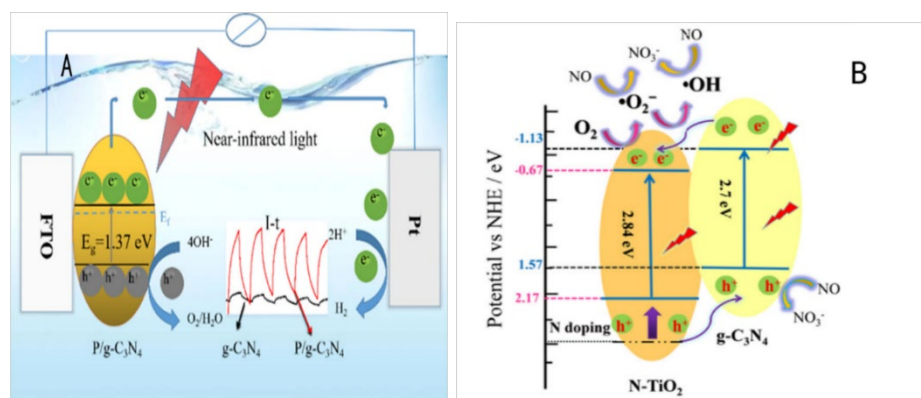


Figure 7: (A) Possible photocatalytic mechanism over P/ g-C<sub>3</sub>N<sub>4</sub> heterojunction<sup>[8]</sup>. (B) Possible photocatalytic mechanism over N-TiO<sub>2</sub>/g-C<sub>3</sub>N<sub>4</sub> heterojunction<sup>[9]</sup>.

## 4. Conclusions

The following conclusions may be made after looking at a number of publications on the use of g-C<sub>3</sub>N<sub>4</sub> in ion doping and hydrogen production. Firstly, it has been demonstrated that ion doping is a useful tactic for greatly enhancing g-C<sub>3</sub>N<sub>4</sub>'s photocatalytic activity. The electrical and energy band structures of g-C<sub>3</sub>N<sub>4</sub> may be tuned by varying the kind and quantity of dopant ions, which enhances the material's capacity to absorb light and the effectiveness of photogenerated carrier separation. Second, there is a wide range of potential applications for g-C<sub>3</sub>N<sub>4</sub>, a nonmetallic photocatalyst, in the hydrogen generation

industry. It is an effective material for visible light-driven hydrogen generation because of its distinct two-dimensional structure and light-responsive qualities. Nevertheless, there are still several obstacles that need to be overcome in order to improve photocatalytic stability and repeatability, including a thorough knowledge of the doping process. We will keep researching g-C<sub>3</sub>N<sub>4</sub> in the areas of hydrogen generation and ion doping.

It is possible to enhance the photocatalytic efficiency of g-C<sub>3</sub>N<sub>4</sub> by investigating novel ion doping techniques and material composite approaches.

Thorough investigation of g-C<sub>3</sub>N<sub>4</sub>'s photocatalytic mechanism and surface reaction kinetics will contribute to elucidating the fundamental causes of its effective hydrogen production and offer theoretical direction for the development of more effective hydrogen production systems.

Furthermore, integrating g-C<sub>3</sub>N<sub>4</sub> with additional functional elements to create a composite photocatalytic system is a significant avenue for further investigation.

It is anticipated that more effective and stable g-C<sub>3</sub>N<sub>4</sub>-based photocatalysts will be developed by the thorough use of techniques including ion doping, material composites, and nanostructure design, which will support the development of the hydrogen energy economy.

### Acknowledgements

This work was supported by the Scientific Research Fund of Hunan Provincial Education Department (Grant No.23A0355) and (Grant No.23B0482).

### References

- [1] Yinhong Qi. *Research on the Construction of Non-Noble Metal Cocatalyst Modified g-C<sub>3</sub>N<sub>4</sub> Based on MOFs and Its Photocatalytic Hydrogen Production Performance [D]*. Qingdao University of Science and Technology, 2021. DOI:10.27264/d.cnki.gqdhc.2020.000790.
- [2] Bi L, Liang X, Zhang L, et al. *The study of photogenerated charge behavior and photocatalytic hydrogen evolution on g-C<sub>3</sub>N<sub>4</sub> decorated with PtCo bimetal[J]*. *Journal of Alloys and Compounds*, 2021, 853: 156843.
- [3] Han Xin, Liu Q, Qian A, et al. *Transition-Metal Single Atom Anchored on MoS<sub>2</sub> for Enhancing Photocatalytic Hydrogen Production of g-C<sub>3</sub>N<sub>4</sub> Photocatalysts[J]*. *ACS Applied Materials & Interfaces*, 2023.
- [4] Pan J, Guan Y, Zhang Y, et al. *Near-Infrared-Induced Photothermal Enhanced Photocatalytic H<sub>2</sub> Production for 3D/2D Heterojunctions of Snowflake-like CuS/g-C<sub>3</sub>N<sub>4</sub> Nanosheets[J]*. *Inorganic Chemistry*, 2022, 62(1): 624-635.
- [5] Yan P, Yuan L, Zhao N, et al. *Constructing novel NaLiTi<sub>3</sub>O<sub>7</sub>/g-C<sub>3</sub>N<sub>4</sub> Z-scheme photocatalysts to facilitate the separation of charge carriers and study the hydrogen production performance[J]*. *New Journal of Chemistry*, 2023, 47(31): 14808-14813.
- [6] Hai T, Chaturvedi R, Mostafa L, et al. *Designing g-C<sub>3</sub>N<sub>4</sub>/ZnCo<sub>2</sub>O<sub>4</sub> nanocomposite as a promising photocatalyst for photodegradation of MB under visible-light excitation: response surface methodology (RSM) optimization and modeling[J]*. *Journal of Physics and Chemistry of Solids*, 2024, 185: 111747.
- [7] Bharathi P, Chidhambaram N, Thirumurugan A. *Conjoining Fe<sub>2</sub>O<sub>3</sub> and g-C<sub>3</sub>N<sub>4</sub> semiconductors to form Fe<sub>2</sub>O<sub>3</sub>/g-C<sub>3</sub>N<sub>4</sub> nanocomposites for photocatalytic applications: An in situ integration approach[J]*. *Journal of Materials Research*, 2023, 38(21): 4736-4746.
- [8] Wu F, Ma Y, Hu Y H. *Near infrared light-driven photoelectrocatalytic water splitting over P-doped g-C<sub>3</sub>N<sub>4</sub> [J]*. *ACS Applied Energy Materials*, 2020, 3(11): 11223-11230.
- [9] Jiang G, Cao J, Chen M, et al. *Photocatalytic NO oxidation on N-doped TiO<sub>2</sub>/g-C<sub>3</sub>N<sub>4</sub> heterojunction: Enhanced efficiency, mechanism and reaction pathway[J]*. *Applied Surface Science*, 2018, 458: 77-85.